Int J Clin Exp Med 2018;11(7):6767-6775
www.ijcem.com /ISSN:1940-5901/IJCEM0069942

Original Article

Role of Bcl-2 antisense oligonucleotides coated by ultrasound microbubble contrast agents in multidrug-resistant MCF-7/ADM breast cancer cells under ultrasonic irradiation

Ai-Qing Lu[1*], Bin Lv[1*], Qin Zhang[2], Xiao-Yun Wang[3], Shu-Xiang Zhang[2]

Departments of [1]Ultrasound, [2]Oncology, [3]Neonatal Intensive Care Unit, Jining No. 1 People's Hospital, Jining, P. R. China. [*]Equal contributors.

Received November 27, 2017; Accepted May 9, 2018; Epub July 15, 2018; Published July 30, 2018

Abstract: Background: Multi-drug resistance (MDR) is a major obstacle for chemotherapeutic treatment of various human cancers, including breast cancer, and many studies have attempted to find an effective way to overcome it. Thus, this study aimed to investigate the role of bcl-2 antisense oligonucleotides (ASODN) combined with ultrasound microbubble contrast agents (UMCA) in MDR mammary carcinoma (MCF-7)/adriamycin (ADM) breast cancer cells under ultrasonic irradiation (UI). Methods: Human breast cancer cell line MCF-7/ADM was used for model establishment and then classified into control, ASODN + liposome + ultrasound irradiation (ASODN + L + UI), and ASODN + ultrasound microbubble contrast agents + UI (ASODN + UMCA + UI) groups. Cell counting method was conducted to detect cell growth. RT-qPCR was performed to measure mRNA expression of multidrug resistance gene-1 (MDR-1) and ATP binding cassette transporter G2 (ABCG2). Protein expression of p-glycoprotein (P-gp) and ABCG2 was detected using Western blotting. Rhodamine 123 was selected to detect P-gp transport function. MTT assay and gel electrophoresis of DNA were conducted to detect cell inhibitory rate and cell apoptosis, respectively. Results: Compared with the control group, ASODN + L + UI and ASODN + UMCA + UI groups showed decreased MCF-7/ADM cell growth, mRNA expression of MDR-1 and ABCG2, and protein expression of P-gp and ABCG2, but increased rhodamine 123 fluorescence intensity, cell apoptosis, and cell inhibitory rates of cells after ADM treatment. Compared with the ASODN + L + UI group, MCF-7/ADM cell growth, mRNA expression of MDR-1 and ABCG2, and protein expression of P-gp and ABCG2 were significantly decreased but rhodamine 123 fluorescence intensity and inhibitory rates were remarkably increased in the ASODN + UMCA + UI group after ADM treatment. Conclusion: This present study provides evidence that Bcl-2 ASODN can reverse MDR in MCF-7/ADM breast cancer cells by downregulating expression of multidrug-resistance-related genes and proteins and inhibiting cell growth, thereby increasing cell sensitivity to ADM.

Keywords: Bcl-2, antisense oligonucleotides, ultrasound microbubble contrast agents, breast cancer, multidrug-resistance, ultrasound irradiation

Introduction

Breast cancer, with micro-calcification clusters and masses as signs, is the second leading reason for cancer deaths in women. Early detection can remarkably reduce the mortality rate but it is usually difficult to differentiate normal breast tissues from abnormalities due to their ambiguous margins [1]. About 30% of breast cancer patients can be explained by risk factors. One study has shown a relationship between exposure to contaminants and incidence of breast cancer [2]. It has remained an ongoing challenge to understand the resistance foundation for identification of novel potential therapeutic targets for breast cancer [3]. Multidrug resistance (MDR) in tumors, a major cause of significant treatment failure, has been observed in studies revealing that article carriers could provide benefits for cancer treatment, including the capability to target tumors and offering opportunities to deal with drug resistance [4]. In cancer, MDR refers to the phenomenon whereby cancer cells become structurally

resistant to unrelated anticancer drugs, bringing altered drug metabolism, reduced apoptosis, drug inactivation, advanced DNA damage repair mechanisms, and overexpression or mutation of the drug's targets [5]. Apoptosis genes, Bcl-2 and Bax, have been detected for analyzing resistant mechanisms and their own drug-specific changes [6].

Bcl-2, an anti-apoptotic gene, is often overexpressed in human cancers and G3139, an antisense oligonucleotide (ASODN) against bcl-2, has shown efficacy for clinical treatment [7]. It has been reported that ASODN, by targeting growth regulatory proteins, performs in prostate cancer models both *in vitro* and *in vivo* [8]. Anti-apoptotic Bcl-2 protein overexpression has been found in solid and hematological tumors, which relates to upregulated resistance fighting against cytotoxic therapy [9]. In addition, ultrasound microbubble contrast agents (UMCA) have also been reported to have potential to significantly enhance treatment of gene therapy by upregulating therapeutic DNA delivery to malignant tissues, which can mechanically perturb cell membranes and blood vessel walls, promoting drug permeability [10]. They have been demonstrated in a variety of clinical, as well as preclinical, ultrasound images [11]. In recent years, coated microbubbles as agents have been applied for quantitative imaging applications due to their accurate theoretical characterization [12]. A previous study examined the differences of doxorubicin-resistant MCF-7/ADM breast cancer cells and doxorubicin-sensitive cells to explore treatment for breast cancer stem cells [13]. Thus, this present study was dedicated to exploring the mechanisms of ASODN combined with UMCA in MDR of MCF-7/ADM breast cancer cells under ultrasonic irradiation (UI).

Materials and methods

Study subjects and model establishment

Anti-adriamycin MCF-7/ADM breast cancer cells, purchased from the US National Cancer Institute (Rockville, Maryland, USA), were maintained in a RPMI-1640 medium containing 10% fetal bovine serum (FBS), 100 μL/mL penicillin, and 100 μL/mL streptomycin (all purchased from Hyclone company, Los Angeles, USA) and then cultured in an 5% CO_2 incubator at 37°C. Cells at logarithmic growth phase were seeded into 6-well plates, followed by addition of serum-free and antibiotic-free RPMI-1640 medium with concentration adjusted to 10^6 cells/mL. Samples were assigned into the control (received no treatment or UI), ASODN + Lipofectamine (L) + UI, and ASODN + UMCA + UI groups. The ASODN + L + UI group was transfected with an intermixture (1:3) of Bcl-2 ASODN (sequence: 5'-AATCCTCCCCCAGTTCACCC-3', 4 μg/mL) and Lipofectamine (Invitrogen Inc., Carlsbad, CA, USA). UI was also conducted (GCZZ type ultrasonic gene transfection therapeutic apparatus, with frequency of 0.3 MHz, pulse ratio of 60%, sound intensity of 0.75 W/cm^2, and total dose of 3.28 J/cm^2). The ASODN + UMCA + UI group was transfected with an intermixture (1:3) of Bcl-2 ASODN and UMCA (0.8-1.8 × 10^9 cells/mL, purchased from Wright Bolaike company, Swiss Confederation), and UI was conducted. Lipofectamine transfection was in strict accordance with kit instructions. Transfected cells were cultured for 6 hours in a serum-free and antibiotic-free RPMI-1640 medium, followed by the medium containing serum.

Detection of cell growth

Cells of the three groups at logarithmic growth phase were selected and digested with 0.25% trypsin. The cell suspension was seeded into 24-well plates and 10^4 cells were seeded into each well. Cells were cultured in a 5% CO_2 incubator for 12 hours at 37°C until cells adhered to the wall. Three wells of cells were made to single cell suspension with 0.25% trypsin every day and they were stained with trypan blue (purchased from Sigma-Aldrich Chemical Company, St Louis MO, USA) and counted for 6 days, consecutively. Cell growth curve of each group was delineated.

Reverse transcription quantitative polymerase chain reaction (RT-qPCR)

Cells of each group were collected and total RNA was extracted by TRIzol (Invitrogen, Carlsbad, California, USA). RNA (500 ng) was reversely transcribed, according to instructions of the Reverse Transcription System A3500 reverse transcription Kit (Promega Corp., Madison, Wisconsin, USA). According to published sequences in GenBank, Primer 5.0 software was used to design primers, which were synthesized by Shanghai Sangon Biotech Co., Ltd

Table 1. Primer sequences for RT-qPCR

Primer	Sequence
β-actin	F: CTACAATGAGCTGCGTGTGGC
	R: CAGGTCCAGACGCAGGATGGC
MDR-1	F: ACTGAGCCTGGAGGTGAAGA
	R: CCACCAGAGAGCTGAGTTCC
ABCG2	F: GGAACTCAGTTTATCCGTGG
	R: GAGCCTACAACTGGCTTAGACTCAA

Note: MDR-1, multidrug resistance gene-1; ABCG2, ATP binding cassette transporter G2; RT-qPCR, reverse transcription quantitative polymerase chain reaction; F, forward; R, reverse.

(Shanghai, China) (**Table 1**). The reaction conditions of RT-qPCR (SYBR Green) were as follows: pre-denaturation at 95°C for 15 minutes, followed by 40 cycles of denaturation at 95°C for 30 second, annealing at 55°C for 30 seconds, and extension at 72°C for 45 seconds. Reaction system included 12.5 μL of Premix Ex Taq or SYBR Green Mix, 1 μL of forward primer, 1 μL of reverse primer, 1-4 μL of DNA template, and up to 25 μL of ddH_2O. β-actin was used as the internal reference and the control group was set as one. Ct value (Power curve of amplification inflection point) of each target gene was obtained. According to Relative Quantification (RQ) = $2^{-\Delta\Delta Ct}$, relative expression value was calculated, with RQ value used for statistical analysis. Instrumentation for RT-qPCR was purchased from BioRad Co., Ltd (iQ5, CA, USA).

Western blotting

Cell proteins of each group were extracted. Protein concentrations were measured using bicinchoninic acid (BCA) Kit (Beyotime Biotechnology Co. Ltd., Shanghai, China). Protein was added to 5 × sample buffer (Beyotime Biotechnology Co. Ltd., Shanghai, China) and boiled at 95°C for 10 minutes, 30 μg of which was added to each well and electrophoretic separation was carried out with 10% polyacrylamide gel (Wuhan Boster Biological Technology Co. Ltd. Wuhan, Hubei, China). Samples were transferred to polyvinylidene fluoride (PVDF) membranes (Amresco Inc., Solon, Ohio, USA). Then, 5% bovine serum albumin (BSA) (Beijing Huamei bioengineering company, Beijing, China) was used to seal at room temperature for 1 hour. After adding primary antibody β-actin (ab8226, 1:1000), p-glycoprotein (P-gp, ab10-3477, 1:500), and ABCG2 (ab63907, 1 μg/mL), all purchased from Santa Cruz Biotechnology, Inc. (California, USA), membranes were washed with Tris-buffered saline tween (TBST) (Beijing Baiaolaibo Technology Co. Ltd, Beijing, China) three times. Finally, proteins were placed at 4°C overnight. Corresponding secondary antibodies (Santa Cruz Biotechnology, Inc., California, USA) were added and the reaction lasted for 2 hours at 37°C. Membranes were then washed again and substrate color A and B (1:1, Promega Corp., Madison, Wisconsin, USA) was added, after being developed at room temperature for 1 minute. Proteins were wrapped in a plastic film, transferred to a darkroom, developed, and fixed by exposure of the X-ray. Gel-Pro analyzer 4.0 software was used to perform band analysis. The ratio of the gray value of target proteins to the gray value of β-actin was used for protein expression. A decolorization table (ZD-9500) was purchased from Taicang Hua Lida Experimental Equipment Co. Ltd. (Jiangsu, China) as well as a vertical transfer electrophoresis tank from Bio-Rad Company (Hercules, CA, USA).

Detection of P glycoprotein transport function

Cells in logarithmic growth phase were chosen and made into single cell suspensions by 0.25% trypsin digestion. The suspensions were incubated in 200 ng/mL Rhodamine 123 solution (Huamei bioengineering company, Beijing, China) at 37°C for 1 hour and then centrifuged for 5 minutes at 1500 rpm. Afterward, the cells were collected. Hanks (Sigma-Aldrich Chemical Company, St Louis MO, USA) was used to wash cell precipitation twice. The cells, incubated again in a RPMI-1640 medium at 37°C for 30 minutes, were collected. Each step was repeated three times. FACSCalibur flow cytometry (Becton, Dickinson and Company, NJ, USA) was applied to determine fluorescence intensity of rhodamine 123 in the cells.

Detection of cell apoptosis and assessment of MDR

Cells in the control, ASODN + L + UI, and ASODN + UMCA + UI groups were collected. ADM, (purchased from Sigma-Aldrich Chemical Company, St Louis MO, USA) with a final concentration of 1 μmol/L was added to the cells. After 48 hours, DNA was extracted in accordance with DNA extraction Kit (purchased from QIAGEN

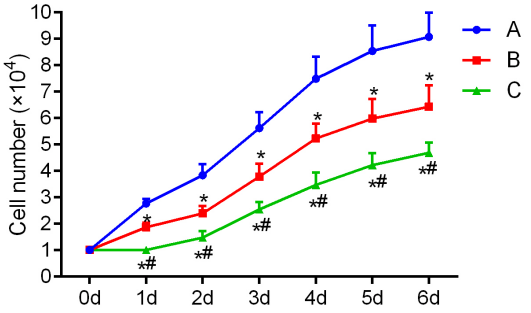

Figure 1. Cells in the control group increased in the first 4 days and entered stable stage on the 5th and 6th day. Cells in the ASODN + UMCA + UI group were much more obviously inhibited. Note: A, the control group; B, the ASODN + L + UI group; C, the ASODN + UMCA + UI group; *, $P < 0.05$, compared with the control group; #, $P < 0.05$, compared with the ASODN + L + UI group; ASODN, antisense oligonucleotide; L, liposome; UI, ultrasound irradiation; UMCA, ultrasound microbubble contrast agents.

Company, Hilden, Germany) instructions. Cell apoptosis was detected by 2% agarose gel electrophoresis. Cells in the control, ASODN + L + UI, and ASODN + UMCA + UI groups were collected again, with the addition of ADM (final concentration of 1 μmol/L), and incubated for 24 hours, 48 hours, and 72 hours after treatment, respectively. Cells in the logarithmic growth phase were collected and seeded into 96-well plates (2×10^4 cells/well), with control well and zero well set. Cells were incubated for 24 hours, then 20 μL of MTT solution (5 mg/mL, purchased from Sigma-Aldrich Chemical Company, St Louis MO, USA) was added to each well for incubation at 37°C for 4 hours. Supernatant in the wells was removed, followed by 150 μL of Dimethyl Sulphoxide (DMSO) oscillating for 10 minutes. Optical density (OD) values were measured at the wavelength of 490 nm by a microplate reader (Bio-Rad, Inc., CA, USA). Each step was repeated three times. The inhibitory rate of cells = $[1 - (OD490_{\text{experimental group}} - OD490_{\text{zero set}})/(OD490_{\text{control group}} - OD490_{\text{zero set}})] \times 100\%$.

Statistical analysis

Statistical analysis was conducted using SPSS 21.0 (IBM Corp. Armonk, NY, USA). Measurement data are presented as mean ± standard deviation. One-way analysis of variance (ANOVA) with Least Significant Difference (LSD) test was exhibited for multi-group comparisons, while *t*-test was applied for differences in one group. *P* values of less than 0.05 were regarded as statistically significant.

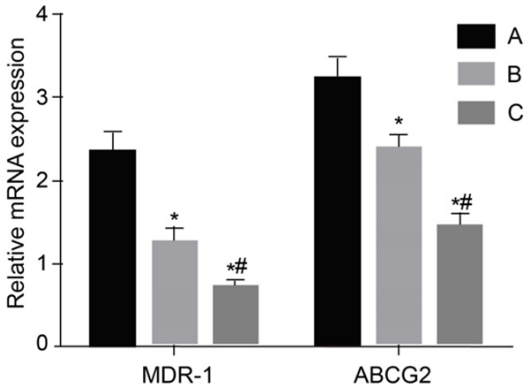

Figure 2. ASODN + MUCA + UI group showed the lowest MDR-1 and ABCG2 mRNA expression. Note: A, the control group; B, the ASODN + L + UI group; C, the ASODN + UMCA + UI group; *, $P < 0.05$, compared with the control group; #, $P < 0.05$, compared with the ASODN + L + UI group; ASODN, antisense oligonucleotide; L, liposome; UI, ultrasound irradiation; UMCA, ultrasound microbubble contrast agents; MDR-1; multidrug-resistance-1; ABCG2, ATP binding cassette transporter G2.

Results

Cells in the control group increased in the first 4 days and entered stable stage on the 5th and 6th days while cells in the ASODN + UMCA + UI group were much more inhibited

The initial cell concentration was 1×10^4 in the three groups. In the control group, cells grew slowly in the first 12 hours and then a rapid growth of cells was observed, reaching the maximum growth rate on the 4th day and remaining stable on the 5th and 6th days. Compared with the control group, cell growth was significantly inhibited in the ASODN + L + UI and ASODN + UMCA + UI groups (both $P < 0.05$). Cell growth in the ASODN + UMCA + UI group was suppressed in a much more remarkable way, compared with ASODN + L + UI group ($P < 0.05$), shown in **Figure 1**. Overall, this experiment indicated that cells in the control group increased in the first 4 days and entered stable stage on the 5th and 6th days, while cells in the ASODN + UMCA + UI group were much more obviously inhibited.

ASODN + MUCA + UI group shows the lowest MDR-1 and ABCG2 mRNA expression and lowest P-gp and ABCG2 protein expression

RT-qPCR was applied to measure mRNA expression of MDR-1 and ABCG2. According to RT-qPCR results (**Figure 2**), compared with the control group, mRNA expression of MDR-1 and

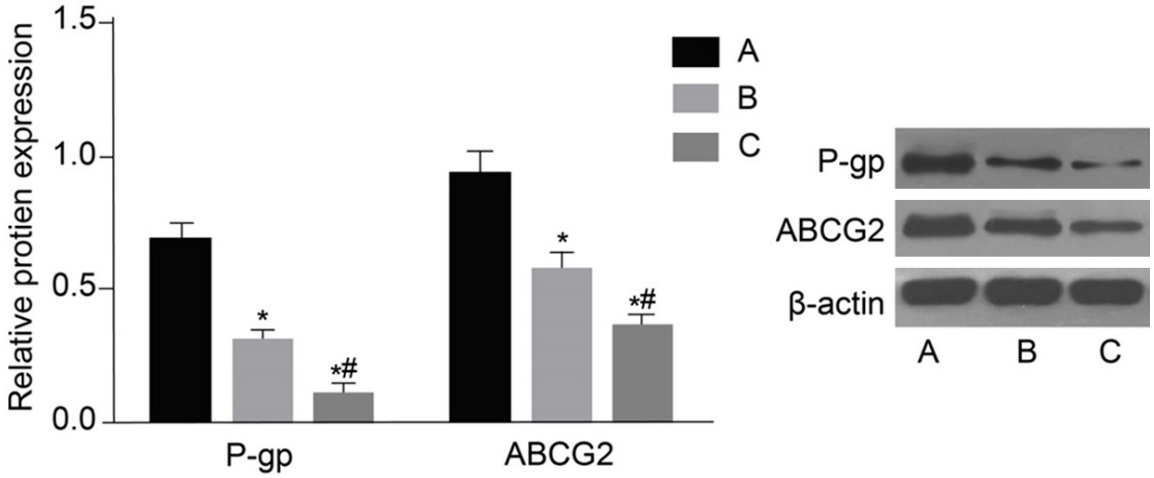

Figure 3. ASODN + MUCA + UI group showed the lowest P-gp and ABCG2 protein expression. Note: A, the control group; B, the ASODN + L + UI group; C, the ASODN + UMCA + UI group; *, $P < 0.05$, compared with the control group; #, $P < 0.05$, compared with the ASODN + L + UI group; ASODN, antisense oligonucleotide; L, liposome; UI, ultrasound irradiation; UMCA, ultrasound microbubble contrast agents; P-gp, p-glycoprotein; ABCG2, ATP binding cassette transporter G2.

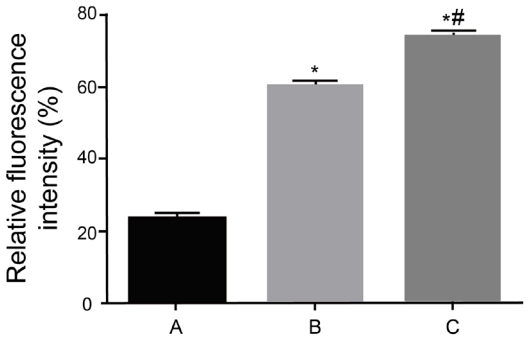

Figure 4. ASODN + UMCA + UI group exhibited the highest rhodamine 123 fluorescence intensity. Note: A, the control group; B, the ASODN + L + UI group; C, the ASODN + UMCA + UI group; *, $P < 0.05$, compared with the control group; #, $P < 0.05$, compared with the ASODN + L + UI group; ASODN, antisense oligonucleotide; L, liposome; UI, ultrasound irradiation; UMCA, ultrasound microbubble contrast agents.

ABCG2 were significantly decreased in the ASODN + L + UI and ASODN + UMCA + UI groups (both $P < 0.05$), while the ASODN + MUCA + UI group exhibited the lowest MDR-1 and ABCG2 mRNA expression. According to Western blotting results (**Figure 3**), protein expression of P-gp and ABCG2 were significantly reduced in ASODN + L + UI and ASODN + UMCA + UI groups (both $P < 0.05$). The ASODN + UMCA + UI group had the lowest protein expression of P-gp and ABCG2. Thus, it was concluded that ASODN + MUCA + UI group showed the lowest MDR-1 and ABCG2 mRNA expression and lowest P-gp and ABCG2 protein expression.

ASODN + UMCA + UI group exhibited the highest rhodamine 123 fluorescence intensity

Flow cytometry was performed to detect P-gp transport function. According to results (**Figure 4**), rhodamine 123 fluorescence intensity in the control group was 23%, while that in the ASODN + L + UI and ASODN + UMCA + UI groups were 63% and 75%, respectively, indicating that fluorescence intensity was significantly increased in the ASODN + L + UI and ASODN + UMCA + UI groups compared with the control group (both $P < 0.05$). Compared with the ASODN + L + UI group, fluorescence intensity was elevated in the ASODN + UMCA + UI group ($P < 0.05$). From this experiment, it can be seen that the ASODN + UMCA + UI group exhibited the highest rhodamine 123 fluorescence intensity.

ASODN + L + UI and ASODN + UMCA + UI groups exhibit obvious cell apoptosis

DNA electrophoresis was conducted to measure cell apoptosis. After ADM (1 μmol/L) treatment for 48 hours, there was no significant cell apoptosis in the control group, indicating that MCF-7/MDR cells were ADM-resistant. Obvi-

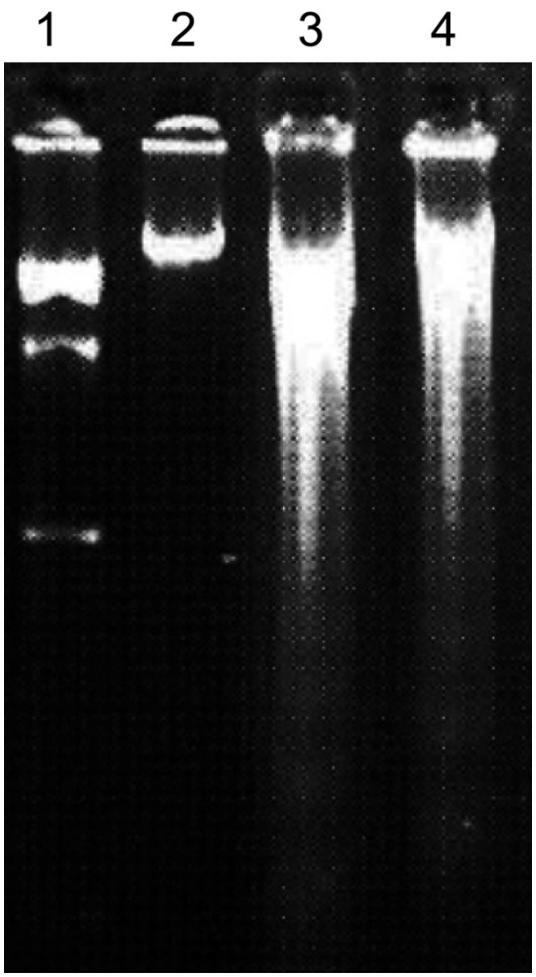

Figure 5. Cell inhibitory rates of the ASODN + UMCA + UI group elevated remarkably. Note: 1, gel electrophoresis image of DNA maker; 2, gel electrophoresis image of the control group; 3, gel electrophoresis image of the ASODN + L + UI group; 4, gel electrophoresis image of the ASODN + UMCA + UI group; *, $P < 0.05$, compared with the control group; #, $P < 0.05$, compared with the ASODN + L + UI group; ASODN, antisense oligonucleotide; L, liposome; UI, ultrasound irradiation; UMCA, ultrasound microbubble contrast agents.

ous cell apoptosis, however, was observed in ASODN + L + UI and ASODN + UMCA + UI groups with ladder bands observed in 2% DNA agar gel electrophoresis (**Figure 5**). Overall, ASODN + L + UI and ASODN + UMCA + UI groups exhibited obvious cell apoptosis.

The cell inhibitory rate of the ASODN + UMCA + UI group is elevated

Cell inhibitory rates, after ADM treatment, were determined by MTT assay. All cells in the control, ASODN + L + UI, and ASODN + UMCA + UI groups were treated with 1 μmol/L ADM for 24 hours, 48 hours, and 72 hours, respectively. Inhibitory rates of cells after 48 hours and 72 hours of ADM treatment were increased significantly compared with that of cells treated with 1 μmol/L ADM for 24 hours (both $P < 0.05$). Compared with the control group, inhibitory rates in the ASODN + L + UI and ASODN + UMCA + UI groups were increased remarkably and the ASODN + UMCA + UI group showed higher inhibitory rates than ASODN + L + UI group (ALL $P < 0.05$), shown in **Table 2**. Therefore, the ASODN + UMCA + UI group revealed upregulated inhibitory rates.

Discussion

Breast cancer is a disease with a distinct metastatic pattern involving regional lymph nodes, bone marrow, lungs, and the liver [14]. Patients suffering from breast cancer have been reported to have markedly different treatment responses and overall outcomes, even in the same stage of the disease [15]. MDR increases the difficulty of breast cancer treatment [16]. UI of cells can exert effectiveness for enhancement of drug targeting, elevating drug absorption rates, and lowering systemic drug toxicity [17]. Interestingly, one study investigated the mechanisms of how UMCA, in the treatment of hepatic cancer, mediated suicide gene transfection, showing a result that suicide genes mediated by MCAs followed by ultrasound therapy can suppress cancer growth *in vivo*, inducing cancer cell apoptosis [18]. It has been proven that the effects of ASODN are affected by its route of cellular uptake [19]. ASODN transfection efficiency has been reported to be positively influenced by each of these four factors: wave intensity, ultrasound duration, gas-filled liposome concentration, and HA2741 concentration [20]. It has been demonstrated that, through transfecting the ultrasonic microbubble intensifier combined with low intensity ultrasound radiation, MDR genes ASODN may serve as a new treatment for hepatocellular carcinoma [21]. This present study demonstrated the good effects of ASODN coated by UMCA on reversal of MDR in breast cancer under UI, possibly serving as a novel treatment strategy for gene therapy.

In this study, MDR-1 and ABCG2 mRNA expression and P-gp and ABCG2 protein expression were significantly reduced in the ASODN +

Table 2. Cell inhibitory rates at different time points of the three groups

Time	Control group	ASODN + L + UI group	ASODN + UMCA + UI group
24 h	1.29 ± 0.17	25.23 ± 1.34*	35.24 ± 1.21$^{*,\#}$
48 h	5.29 ± 0.32$^{\$}$	31.64 ± 1.85$^{*,\$}$	46.83 ± 1.87$^{*,\#,\$}$
72 h	7.31 ± 0.62$^{\$}$	41.96 ± 1.98$^{*,\$}$	56.87 ± 2.15$^{*,\#,\$}$

Note: *, compared with the control group, $P < 0.05$; #, compared with the ASODN + L + UI group, $P < 0.05$; $, compared with 24 h after treatment with adriamycin, $P < 0.05$; ASODN, antisense oligonucleotide; L, liposome; UI, ultrasound irradiation.

UMCA + UI group, indicating that ASODN coated by UMCA inhibited MDR in breast cancer under UI. MDR is a commonly seen phenomenon among ovarian cancer patients which limits its ultimate chemotherapy success in clinical treatment. MDR1 genes and corresponding P-gp are regarded as well-accepted MDR mechanisms [22]. P-gp mediated MDR, a major cause of chemotherapy failure, has been proven to show great potential acting as a therapeutic biomarker for drug-resistant cancer [23]. Chemoresistance, presented as overexpression of MDR1 gene encoding P-gp, is a major obstacle to chemotherapy success for colorectal cancer [24]. One study found that HIF-1α inhibition can reverse MDR by suppressing MDR1/P-gp in colon cancer cells [25]. Another study showed that decreased MDR1 expression could be used to reverse the process of MDR in liver cancer [26]. In addition, BCRP (gene symbol ABCG2), a "half-type" ABC transporter, plays a role as homodimer and transporter of anticancer agents, namely irinotecan, mitoxantrone, imatinib, 7-ethyl-10-hydroxycamptothecin (SN-38), methotrexate, and gefitinib from cells. This can affect metabolism, drug absorption, excretion, and distribution [27]. Also a human breast cancer resistance protein, BCRP/ABCG2 has been found to have pharmacological functions to drug disposition and resistance [28]. It has been further proven that inhibition of ABCG2 can suppress tumor growth by regulating cell apoptosis and proliferation [29]. Leuk Res et al. demonstrated, statistically, that remarkably higher expression of P-gp (5.25% vs 3.48%) and multidrug resistance-associated protein-1 (MRP1) (5.24% vs 3.54%) was observed in treatment-failed patients than responders [30]. Taken together, it can be concluded that ASODN coated by UMCA is able to inhibit MDR in breast cancer under UI.

Increased rhodamine 123 fluorescence intensity was exhibited in the ASODN + UMCA + UI group, suggesting that ASODN coated by UMCA can suppress MDR in breast cancer under UI. Rhodamine 123, a fluorescent cationic dye, is commonly adapted as a mitochondrial and suspected to be transported by some typical drug membrane transporters [31]. In a study on compounds 1-3's effects on reversion of MDR mediated by P-glycoprotein, rhodamine-123 exclusion screening tests were used on human ABCB1 genes [32]. Significant increase in accumulation of rhodamine-123 was observed in a previous study, further warranting the function of MDR reversal agents for clinical anticancer agents [33]. A study by Oncol Lett et al., evaluating different methods of improving resistance to chemotherapeutic drugs, revealed an increased intracellular accumulation of rhodamine 123 [34]. It was found that α- and β-asarone increased rhodamine 123 in Caco-2 cells and declined P-gp mRNA in cells, indicating that α- and β-asarone can reverse MDR by downregulation of P-gp expression and function [35]. Importantly, hypoxic laryngeal carcinoma cell apoptosis rates increased following a decrease in MDR1/P-gp expression and increased intracellular Rh123 accumulation in fluorescence intensity [36]. All of the studies mentioned above were in line with results of this present study, thus, it was easy to conclude that ASODN coated by UMCA increases fluorescence intensity of rhodamine 123, suppressing MDR in breast cancer under UI.

In conclusion, this study provides new insight into mechanisms whereby ASODN coated by UMCA under UI can downregulate expression of multi-drug resistance-related proteins and inhibit cell growth and cell sensitivity to ADM, thus, exerting effects leading to reversal of MDR in breast cancer. This method can be very effective in overcoming drug resistance in the treatment of breast cancer.

Acknowledgements

We would like to acknowledge the reviewers for helpful comments on this paper.

Disclosure of conflict of interest

None.

Address correspondence to: Dr. Shu-Xiang Zhang, Department of Oncology, Jining No. 1 People's Hospital, 6 Jiankang Road, Jining 272011, Shan-

dong Province, P. R. China. Tel: +86-13668828766; E-mail: zhshuxiang@126.com

References

[1] Dheeba J, Albert Singh N, Tamil Selvi S. Computer-aided detection of breast cancer on mammograms: a swarm intelligence optimized wavelet neural network approach. J Biomed Inform 2014; 49: 45-52.

[2] Crouse DL, Goldberg MS, Ross NA, Chen H, Labreche F. Postmenopausal breast cancer is associated with exposure to traffic-related air pollution in Montreal, Canada: a case-control study. Environ Health Perspect 2010; 118: 1578-1583.

[3] Lopez-Knowles E, O'Toole SA, McNeil CM, Millar EK, Qiu MR, Crea P, Daly RJ, Musgrove EA, Sutherland RL. PI3K pathway activation in breast cancer is associated with the basal-like phenotype and cancer-specific mortality. Int J Cancer 2010; 126: 1121-1131.

[4] Yan Y, Bjornmalm M, Caruso F. Particle carriers for combating multidrug-resistant cancer. ACS Nano 2013; 7: 9512-9517.

[5] Hung TH, Hsu SC, Cheng CY, Choo KB, Tseng CP, Chen TC, Lan YW, Huang TT, Lai HC, Chen CM, Chong KY. Wnt5A regulates ABCB1 expression in multidrug-resistant cancer cells through activation of the non-canonical PKA/beta-catenin pathway. Oncotarget 2014; 5: 12273-12290.

[6] Li WJ, Zhong SL, Wu YJ, Xu WD, Xu JJ, Tang JH, Zhao JH. Systematic expression analysis of genes related to multidrug-resistance in isogenic docetaxel- and adriamycin-resistant breast cancer cell lines. Mol Biol Rep 2013; 40: 6143-6150.

[7] Cheng X, Liu Q, Li H, Kang C, Liu Y, Guo T, Shang K, Yan C, Cheng G, Lee RJ. Lipid nanoparticles loaded with an antisense oligonucleotide gapmer against Bcl-2 for treatment of lung cancer. Pharm Res 2017; 34: 310-320.

[8] Rubenstein M, Hollowell CM, Guinan P. Compensatory and non-compensatory effects on protein expression following BCL-2 suppression by antisense oligonucleotides. Med Oncol 2012; 29: 2284-2290.

[9] Wiedenmann N, Koto M, Raju U, Milas L, Mason KA. Modulation of tumor radiation response with G3139, a bcl-2 antisense oligonucleotide. Invest New Drugs 2007; 25: 411-416.

[10] Sirsi SR, Borden MA. Advances in ultrasound mediated gene therapy using microbubble contrast agents. Theranostics 2012; 2: 1208-1222.

[11] Mullin L, Gessner R, Kwan J, Kaya M, Borden MA, Dayton PA. Effect of anesthesia carrier gas on in vivo circulation times of ultrasound microbubble contrast agents in rats. Contrast Media Mol Imaging 2011; 6: 126-131.

[12] O'Brien JP, Stride E, Ovenden N. Surfactant shedding and gas diffusion during pulsed ultrasound through a microbubble contrast agent suspension. J Acoust Soc Am 2013; 134: 1416-1427.

[13] Dong Y, Li L, Wang L, Zhou T, Liu JW, Gao YJ. Preliminary study of the effects of beta-elemene on MCF-7/ADM breast cancer stem cells. Genet Mol Res 2015; 14: 2347-2355.

[14] Muller A, Homey B, Soto H, Ge N, Catron D, Buchanan ME, McClanahan T, Murphy E, Yuan W, Wagner SN, Barrera JL, Mohar A, Verastegui E, Zlotnik A. Involvement of chemokine receptors in breast cancer metastasis. Nature 2001; 410: 50-56.

[15] van 't Veer LJ, Dai H, van de Vijver MJ, He YD, Hart AA, Mao M, Peterse HL, van der Kooy K, Marton MJ, Witteveen AT, Schreiber GJ, Kerkhoven RM, Roberts C, Linsley PS, Bernards R, Friend SH. Gene expression profiling predicts clinical outcome of breast cancer. Nature 2002; 415: 530-536.

[16] Zhang H, Zhang X, Wu X, Li W, Su P, Cheng H, Xiang L, Gao P, Zhou G. Interference of Frizzled 1 (FZD1) reverses multidrug resistance in breast cancer cells through the Wnt/beta-catenin pathway. Cancer Lett 2012; 323: 106-113.

[17] Tachibana K. [Molecular diagnosis and treatment using a new ultrasound contrast agent]. Gan To Kagaku Ryoho 2013; 40: 291-293.

[18] Tang Q, He X, Liao H, He L, Wang Y, Zhou D, Ye S, Chen Q. Ultrasound microbubble contrast agent-mediated suicide gene transfection in the treatment of hepatic cancer. Oncol Lett 2012; 4: 970-972.

[19] Alam MR, Ming X, Dixit V, Fisher M, Chen X, Juliano RL. The biological effect of an antisense oligonucleotide depends on its route of endocytosis and trafficking. Oligonucleotides 2010; 20: 103-109.

[20] Luo YK, Zhao YZ, Lu CT, Tang J, Li XK. Application of ultrasonic gas-filled liposomes in enhancing transfer for breast cancer-related antisense oligonucleotides: an experimental study. J Liposome Res 2008; 18: 341-351.

[21] Jiang MD, Peng ZP, Li SL, Wang ZG, Ran HT, Huo SH, Yin XL. [Reversion of multidrug resistance of hepatocellular carcinoma by antisense oligonucleotides and ultrasonic microbubble intensifier transfection combined with ultrasound irradiation]. Zhonghua Gan Zang Bing Za Zhi 2006; 14: 341-345.

[22] Yang X, Iyer AK, Singh A, Choy E, Hornicek FJ, Amiji MM, Duan Z. MDR1 siRNA loaded hyaluronic acid-based CD44 targeted nanoparticle

systems circumvent paclitaxel resistance in ovarian cancer. Sci Rep 2015; 5: 8509.
[23] Yhee JY, Song S, Lee SJ, Park SG, Kim KS, Kim MG, Son S, Koo H, Kwon IC, Jeong JH, Jeong SY, Kim SH, Kim K. Cancer-targeted MDR-1 siRNA delivery using self-cross-linked glycol chitosan nanoparticles to overcome drug resistance. J Control Release 2015; 198: 1-9.
[24] Liu Z, Duan ZJ, Chang JY, Zhang ZF, Chu R, Li YL, Dai KH, Mo GQ, Chang QY. Sinomenine sensitizes multidrug-resistant colon cancer cells (Caco-2) to doxorubicin by downregulation of MDR-1 expression. PLoS One 2014; 9: e98560.
[25] Chen J, Ding Z, Peng Y, Pan F, Li J, Zou L, Zhang Y, Liang H. HIF-1alpha inhibition reverses multidrug resistance in colon cancer cells via downregulation of MDR1/P-glycoprotein. PLoS One 2014; 9: e98882.
[26] Zhou JJ, Deng XG, He XY, Zhou Y, Yu M, Gao WC, Zeng B, Zhou QB, Li ZH, Chen RF. Knockdown of NANOG enhances chemosensitivity of liver cancer cells to doxorubicin by reducing MDR1 expression. Int J Oncol 2014; 44: 2034-2040.
[27] Noguchi K, Katayama K, Sugimoto Y. Human ABC transporter ABCG2/BCRP expression in chemoresistance: basic and clinical perspectives for molecular cancer therapeutics. Pharmgenomics Pers Med 2014; 7: 53-64.
[28] Mao Q, Unadkat JD. Role of the breast cancer resistance protein (BCRP/ABCG2) in drug transport--an update. AAPS J 2015; 17: 65-82.
[29] Xie J, Jin B, Li DW, Shen B, Cong N, Zhang TZ, Dong P. ABCG2 regulated by MAPK pathways is associated with cancer progression in laryngeal squamous cell carcinoma. Am J Cancer Res 2014; 4: 698-709.
[30] Park SH, Park CJ, Kim DY, Lee BR, Kim YJ, Cho YU, Jang S. MRP1 and P-glycoprotein expression assays would be useful in the additional detection of treatment non-responders in CML patients without ABL1 mutation. Leuk Res 2015; 39: 1109-1116.
[31] Jouan E, Le Vee M, Denizot C, Da Violante G, Fardel O. The mitochondrial fluorescent dye rhodamine 123 is a high-affinity substrate for organic cation transporters (OCTs) 1 and 2. Fundam Clin Pharmacol 2014; 28: 65-77.
[32] Rauf A, Uddin G, Siddiqui BS, Molnar J, Csonka A, Ahmad B, Szabo D, Farooq U, Khan A. A rare class of new dimeric naphthoquinones from diospyros lotus have multidrug reversal and antiproliferative effects. Front Pharmacol 2015; 6: 293.
[33] Karthikeyan C, Malla R, Ashby CR, Jr., Amawi H, Abbott KL, Moore J, Chen J, Balch C, Lee C, Flannery PC, Trivedi P, Faridi JS, Pondugula SR, Tiwari AK. Pyrimido[1",2":1,5]pyrazolo[3,4-b] quinolines: novel compounds that reverse ABCG2-mediated resistance in cancer cells. Cancer Lett 2016; 376: 118-126.
[34] Wang J, Li G. Mechanisms of methotrexate resistance in osteosarcoma cell lines and strategies for overcoming this resistance. Oncol Lett 2015; 9: 940-944.
[35] Meng X, Liao S, Wang X, Wang S, Zhao X, Jia P, Pei W, Zheng X, Zheng X. Reversing P-glycoprotein-mediated multidrug resistance in vitro by alpha-asarone and beta-asarone, bioactive cis-trans isomers from Acorus tatarinowii. Biotechnol Lett 2014; 36: 685-691.
[36] Li D, Zhou L, Huang J, Xiao X. Effect of multidrug resistance 1/P-glycoprotein on the hypoxia-induced multidrug resistance of human laryngeal cancer cells. Oncol Lett 2016; 12: 1569-1574.